

Sputtering Deposition and Characterization of Ru-Doped WO₃ Thin Films for Electrochromic Applications

E. Cazzanelli¹, M. Castriota¹, R. Kalendarev², A. Kuzmin² and J. Purans²

¹Department of Physics, University of Calabria and Unità INFM Cosenza,
I-87036 Arcavacata di Rende, Cosenza, ITALY

²Institute of Solid State Physics, University of Latvia,
Kengaraga street 8, LV-1063 Riga, LATVIA

Abstract. Mixed tungsten-ruthenium oxide thin films were prepared for the first time by dc magnetron co-sputtering technique and were studied by cyclic voltammetry, optical transmission measurements, Raman spectroscopy and the W L₃ and Ru K edges X-ray absorption spectroscopy (XAS) in comparison with pure WO₃ films. The Ru concentration was varied in the range from 0 to 28 at.%. XAS results suggest that the average local structure around both tungsten and ruthenium ions remains unchanged within experimental accuracy in all samples, moreover, for tungsten ions, it resembles that of pure WO₃ films. However, the presence of the ruthenium ions affects the electrochemical and optical properties of the films. Our results suggest that mixed films are formed by tungsten trioxide grains surrounded by ruthenium oxide phase.

1. Introduction

After years of research, tungsten trioxide (WO₃) is still the most used inorganic material for active layer in electrochromic devices [1]. A change of colour upon cation intercalation occurs even in crystalline WO₃, but it is well known that amorphous WO₃ films have faster response time during colouring and bleaching processes. Many different techniques have been employed to produce WO₃ films: sputtering, evaporation and sol-gel methods are the most used ones. It is known that structural characteristics and hereafter the electrochemical performance show an appreciable variability, depending on the production method [2]. Several problems still remain to have reliable and efficient electrochromic devices: the switching speed, the cyclability and the long term degradation are among them. In addition, colours different from the blue can be useful for applications.

An interesting route to improve the quality of active electrochromic layer is doping of WO₃ by other metal oxides. In principle, small amount of another oxide can change (i) the structural properties of tungsten trioxide, thus

promoting or inhibiting the cluster growth during the deposition, and (ii) its electrical conductivity, due to the exchange of electrons between the dopant and the host. In the present work we studied an influence of the co-doping with ruthenium ions on electrochemical, optical and structural properties of tungsten oxide thin films.

2. Experimental Description

2.1. Sample Preparation. All thin film samples were prepared by dc magnetron sputtering technique from metallic targets in mixed Ar/O₂ atmosphere. Various substrates as ITO coated glass, silicon and polyimide film were used. For pure WO₃ films, metallic tungsten target was used. To produce mixed W-Ru oxide films, tungsten target was covered with stripes of metallic ruthenium. A variation of the ratio between areas of tungsten and ruthenium targets was used to change the films composition. Thus, the percentages of ruthenium ions reported in this paper (1, 2, 4, 8 and 16) are actually the surface ratios between the ruthenium metal stripes and the tungsten target. Note that the real composition ratio of two metals in the films is

different, due to the difference in sputtering rate of ruthenium and tungsten. The real composition of the films was determined for samples with high Ru content by X-ray absorption technique from the ratio of the absorption jumps at the W L_3 and Ru K edges. Our results indicate that the metallic ruthenium has about 1.8 times higher sputtering rate than the metallic tungsten in our sputtering conditions. Therefore, for example, the film with the nominal Ru content of 16 % contains, in fact, about 28 at.% of ruthenium. The Ar:O₂ ratio in the sputtering chamber was maintained at the value of 5:1. The pressure during the sputtering process was $5 \cdot 10^{-2}$ Torr, the current 0.12 A and the voltage 600 V. The distance between target and substrate was 8.5 cm. Two series of mixed oxide films with different Ru content were obtained on ITO coated glasses: the first series corresponded to a deposition time of 45 min, the second one to a deposition time of 90 min. As prepared films had a brown-amber colour and appeared homogeneous under optical microscope investigation.

2.2. Electrochemical Characterisation. Cyclic voltammetry measurements (Fig. 1) were performed using conventional set-up, consisting of three electrodes scheme with the Pt counter electrode and the Ag/AgCl reference electrode. A 0.1N aqueous solution of H₂SO₄ was used as an electrolyte. The scanning rate was 50 mV/sec, and all measurements were performed at room temperature. Each I-V curve was taken after 10 to 20 cycles, which were required for a stabilisation of samples response.

2.3. Optical Transmission Measurements. Optical transmission experiments (Fig. 2) were performed using a

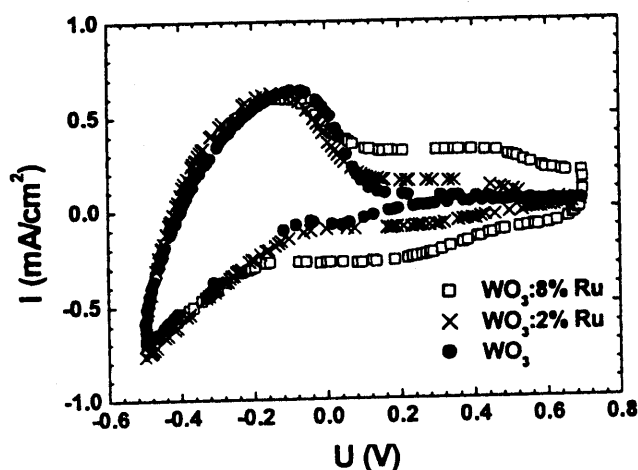


Fig. 1. Cyclic voltammograms of WO₃ films, having increasing Ru content. The percentage indicated in this figure and in the following is a deposition parameter, i.e. the surface percentage of the target covered by Ru metal.

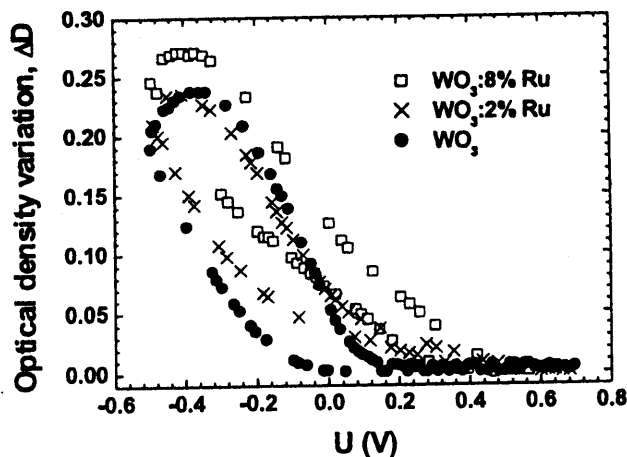


Fig. 2. Optical density measurement of the same films as in Fig. 1. The variation of the optical density of the samples is plotted versus the applied voltage during the cyclic voltammetry measurement.

simple setup. Transparent electrochemical cell with a sample and electrolyte was placed in the light beam, provided by a 5 mW 650 nm diode laser. The transmitted light was measured by a photodiode. The transmission coefficient was calculated relative to the cell with electrolyte but without the sample. Such setup allowed us to perform simultaneous cyclic voltammetry and transmission measurements.

2.4. Raman Spectroscopy. A Raman microprobe Jobin-Yvon Labram was used, equipped with a CCD detector and a He-Ne laser (632.8 nm emission). In all the experiments the power of the laser out of the objective, a 100× Mplan Olympus with NA of 0.90, was about 5 mW, and the focused laser spot had about 2-3 μm of apparent diameter. By assuming such values of spot diameter and laser power, we have for the unfiltered laser beam an irradiance of the order of 100 kW/cm² on the spot.

For the spectral mapping on the doped films a special X-Y stage for automatic spectral mapping was used. To ensure that no photochemical transformation occurs in the film samples, a time evolution kinetics has been recorded, showing no significant change of shape or intensity in the samples collected after 6 months storage.

The most useful measurement has been performed by using the Z scan option of the apparatus, to obtain different Raman spectra from the substrate and from the deposited films. The depth resolution of the confocal microscope, by using a proper confocal hole diameter (150 μm), is of the order of 1 μm, but in any case is well evident the difference

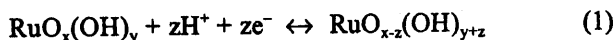
between the substrate spectrum and that of the deposited film. To study the evolution of the spectra for increasing doping concentration, for any Z scan performed on the samples of different composition, the spectra showing the maximum intensity of the 950 cm⁻¹ band, typical of the film, have been chosen.

2.5. X-ray Absorption Spectroscopy. The W L₃- and Ru K-edge X-ray absorption spectra were measured at room temperature at the LURE DCI D21 (XAS-2) beamline (Orsay, France). A standard transmission scheme with a Si(311) double-crystal monochromator and two ion chambers was used. The extended X-ray absorption fine structure (EXAFS) signals above the two edges were extracted and analysed by the EDA software package [3,4] by using a conventional approach. The theoretical back-scattering amplitudes and phases, calculated by the ab initio FEFF6 code [5], were used in the analysis of the first coordination shell around W and Ru ions. The calculations by the FEFF6 code were performed for two clusters, having a structure of crystalline m-WO₃ and RuO₂. Complex exchange-correlation Hedin-Lundqvist potential was employed to account for inelastic losses [5]. The position of the photoelectron energy origin E₀ [6] in the experiment was chosen to match the theoretical one by aligning experimental and theoretical EXAFS spectra in the best way.

3. Results and Discussion

3.1. Cyclic Voltammetry and Optical Transmission Measurements. Cycling voltammograms of the films deposited during 90 min are shown in Fig. 1. An increase of ruthenium content modifies the curves in the positive potential region. Voltammograms of pure WO₃ and mixed films at low doping concentration (1%-4%) differ only slightly in the cathodic region shape. But the shape of voltammograms in anodic region for samples mixed with ruthenium changes progressively and at higher concentrations (8-16%) is similar to the one for pseudo-capacitor [7]. This effect can be related to redox processes between different oxidation states of ruthenium ions.

The high specific capacitance of hydrous ruthenium oxides results from a pseudocapacitive effect whereby both protons and electrons are "double injected" from an acidic electrolyte into the surface of hydrous ruthenium oxide, as described by the equation [8]



During this process the Ru⁴⁺ cation is reduced while the oxygen ion in its site is protonated, thus the full electron/proton reaction can be written as [9]



Here charge is stored and discharged with the concomitant exchange of protons and electrons from the mixed-conducting material. Note that the capacitance of RuO_xH_y has been correlated to several variables, including surface area, water content, electronic conductivity and crystallinity.

An addition of ruthenium in tungsten oxide increases probably the conductivity of material, thus allowing occurrence of redox reactions between two tungsten ion states already at anodic potentials. A comparison of cycling voltammograms (Fig. 1) and optical transmission curves (Fig. 2) allows us to conclude that a change of transmission in pure WO₃, due to a reduction of tungsten ions



starts at 0 V, whereas for 1% Ru content at +0.2 V and for 2-4% Ru at +0.35 V. Further increase of ruthenium content shifts the beginning of colouration toward the cathodic region, so that it occurs at about +0.1 V for 16% Ru. Optical efficiency decreases with increasing ruthenium content from 0.48 cm²/C for pure WO₃ to 0.35 cm²/C for WO₃:8% Ru because of an increase of charge capacity related to the redox processes at ruthenium ions.

3.2. Raman Measurements. The Raman spectrum of the WO₃ films shows an appreciable variability in shape, depending on the crystallinity degree, the amount of water, the porosity of the film. For such reasons different spectra are obtained by using different deposition techniques, or even changing the parameters within a chosen method. However, the common features of the amorphous films are a broad band peaked at slightly below 800 cm⁻¹ and another one at about 950 cm⁻¹, usually attributed to the terminal W-O bonds [10-13]. Our pure WO₃ films, obtained by reactive sputtering with the parameters listed above, show high intensity ratio between the 950 cm⁻¹ band and the broad band at about 800 cm⁻¹, attributed to the bulk W-O bond vibrations. This spectroscopic evidence could indicate a high degree of porosity or a very small size of the WO₃ clusters. In our measurements, the spectrum of the substrate, ITO coated glass, appears very strong, due to the small thickness of the films. To have a good Raman signal,

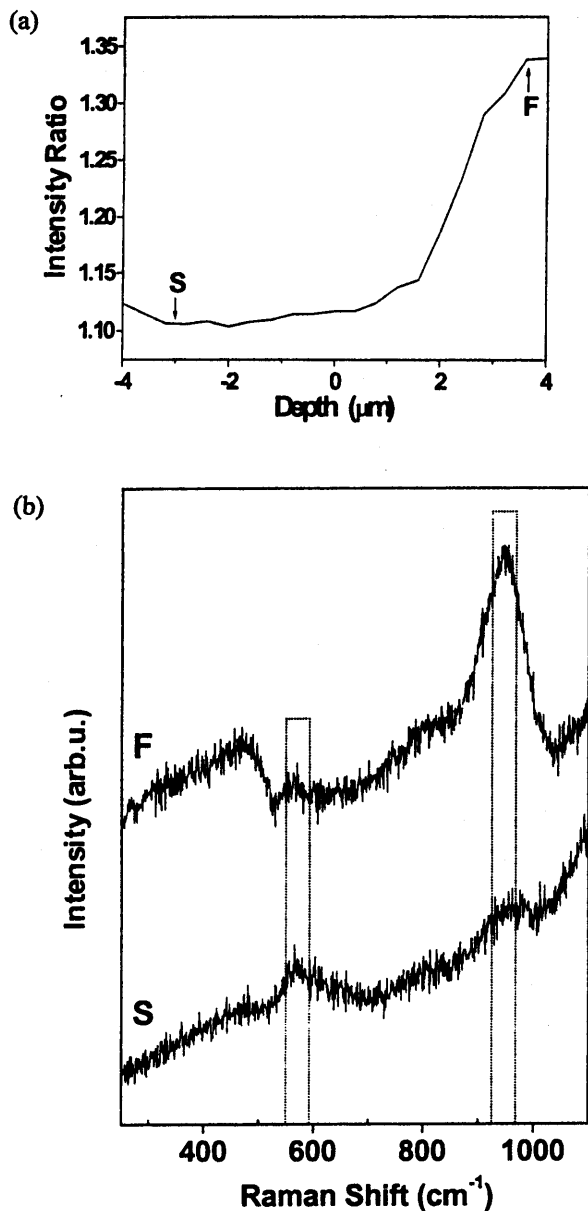


Fig. 3. (a) Z scan of Raman intensity ratio between the highest energy WO_3 peak and the characteristic substrate peak, performed on the film sample with 2% Ru doping, by using a confocal hole diameter of $150 \mu\text{m}$. (b) Typical spectra of the substrate (S) and of the deposited film (F), corresponding to the points of Z scan indicated in that way in Fig. 3(a). The spectral slices used for the intensity ratio are also shown.

independent from the particular focusing on any spot of the film samples, a Z scan has been performed, with vertical steps of $0.5 \mu\text{m}$.

A typical Z scan is depicted in Fig. 3(a). It shows the ratio between two spectral slices: the one (about 50 cm^{-1} wide), centred at the maximum of the W-O terminal bonds

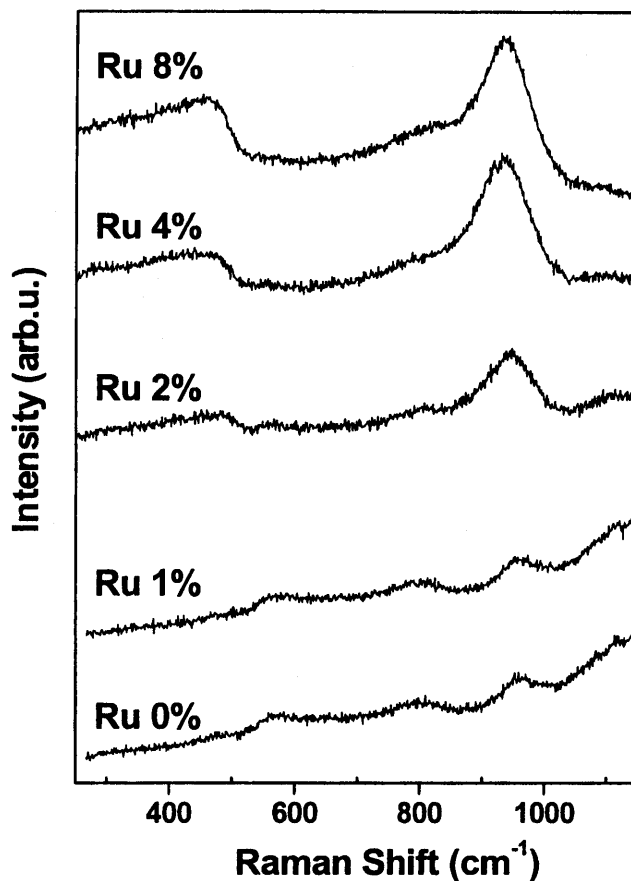


Fig. 4. Evolution of Raman spectral shape of the sputtered WO_3 films versus the Ru content. All spectra correspond to the maximum intensity ratio in the Z scans as that in Fig. 3.

peak, divided by the slice with comparable width, centred at the substrate peak at about 560 cm^{-1} . Two extreme spectra are shown in Fig. 3(b): they represent mostly the substrate (S) contribution and the maximum signal from the deposited film (F), respectively. The spectrum corresponding to the maximum ratio between the signal of the 950 cm^{-1} band and the substrate signal at 560 cm^{-1} was chosen to analyze the dependence of the Raman scattering of the film on the dopant concentration.

The experimental spectra of $\text{WO}_3:\text{Ru}$ samples for all investigated Ru concentrations are shown in Fig. 4, including a pure WO_3 sample for comparison. The films deposited for longer time (90 min) have been chosen for their larger thicknesses, giving a stronger Raman signal, but even the films with expected lower thicknesses show similar behaviour.

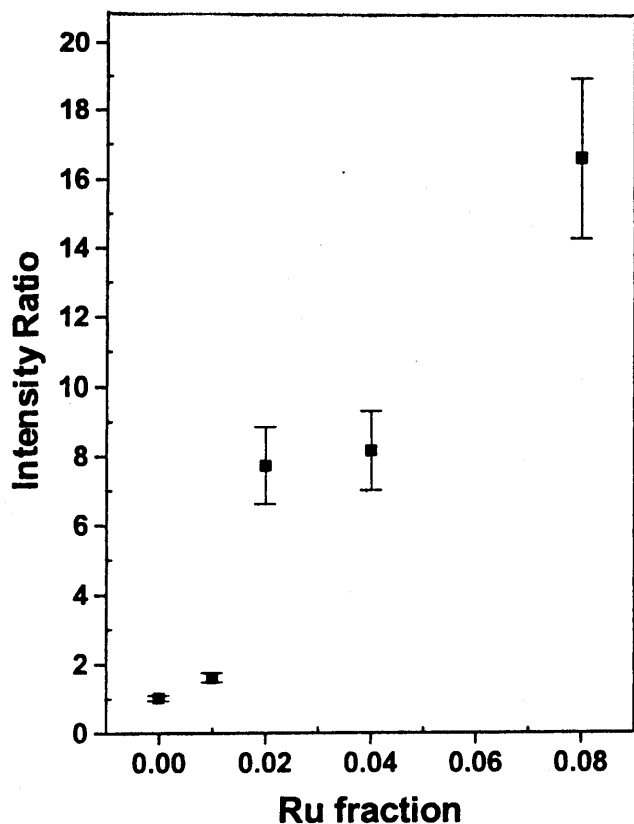


Fig. 5. Intensity ratio between the Raman band for the terminal bonds, at about 950 cm^{-1} and that for bulk W-O bonds, at about 800 cm^{-1} . Error bars derive from the errors of the Gaussian fits.

The most remarkable effect is the strong relative increase of the 950 cm^{-1} band for increasing Ru content. In Fig. 5 the intensity ratios between this band and the other one at about 800 cm^{-1} , also typical of WO_3 , are plotted for the various compositions. The ratios have been obtained by dividing the intensity values given by a Gaussian fit, performed after subtracting a proper baseline. Taking into account the uncertainty of the fit a reasonable linear dependence of the ratio is obtained. The other remarkable evolution of the spectra at higher Ru doping is the change of the shape in the low frequency region: here an asymmetric band, peaked at about 470 cm^{-1} , becomes more and more stronger for increasing doping, while the peak of the substrate at 560 cm^{-1} merges in the continuum background. It is worth to point out that all these spectral features can be assigned to the tungsten trioxide vibrational dynamics. In fact no sharp peak or band resembling the spectrum of RuO_2 is observed.

In particular, the highest frequency band, whose intensity correlates well to the Ru content, does not correspond to any vibrational mode of ruthenium oxide as results from the Raman spectrum of the rutile crystal phase [14] or else of the sputtered films [15,16], because these spectra do not show any peak above 750 cm^{-1} .

The most viable explanations for the change of the spectral shape under increasing Ru content have structural and electronic origin. The presence of ruthenium ions above some concentration threshold, about the nominal 2% in our convention, favours the formation of very small WO_3 clusters, decorated by ruthenium oxide particles. In fact, the low frequency spectrum shows a typical shape of vibrational density of states, which is common for glasses and for a phonon confinement effect. Some Raman scattering enhancement occurs for all vibrational bands, because of the Ru decoration at the interface of WO_3 clusters, but a particular change involves specific vibration mode of the terminal bonds, at about 950 cm^{-1} (Fig. 4). Strong relative increase of this band, which is roughly linear vs. the Ru content, could suggest a specific resonant effect, due to the particular electronic configuration within W-O-Ru chains at the interface of the clusters. A similar evidence has been found in a former study [17,18] on polycrystalline mixtures of $\text{WO}_3\text{-ReO}_2$: a weak Raman resonance effect was detected only in the presence of ReO_2 , for the same W-O terminal bond vibration mode, by exciting in the red light region, and it has been attributed to the electronic configuration of the W-O-Re chain at the microcrystal interface. In that case, the surface-to-volume ratio was smaller, and the high frequency band of the terminal bonds was always lower in intensity in respect to the bulk crystal peak at 800 cm^{-1} . In the present study, very high porosity of the host tungsten oxide and a quite strong resonant effect make the 950 cm^{-1} band the dominant feature in the Raman spectrum of the Ru doped films.

The increasing Ru doping induces also some less evident effect on the spectral parameters of the observed bands. Even taking into account errors in the frequency calibration of the Raman spectrometers, a systematic trend toward lower frequencies is observed for the band at 950 cm^{-1} . It shifts from the value of 958 cm^{-1} for pure WO_3 film down to 932 cm^{-1} for 4% Ru-doped samples. On the contrary, the bulk vibrational band of WO_3 seems to have an upshift of the maximum, from 790 cm^{-1} for pure tungsten oxide up to about 830 cm^{-1} for the highest available doping. However, the low intensity of this band, its large bandwidth and the

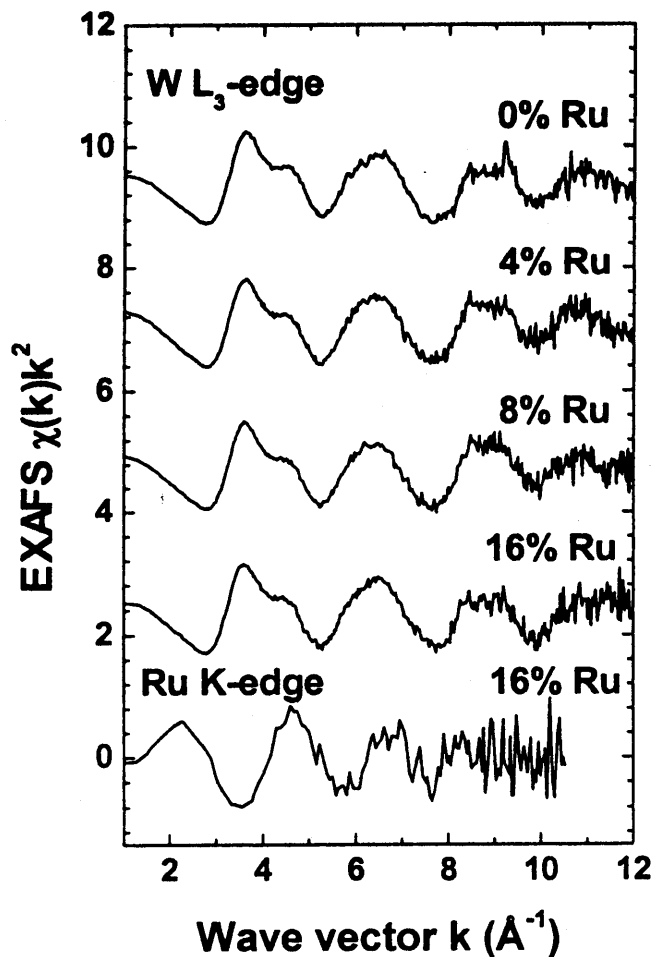


Fig. 6. Experimental EXAFS $\chi(k)k^2$ signals at the $W L_3$ and Ru K edges in pure WO_3 (upper curve) and mixed W-Ru oxide thin films. Note a similarity of signals for the $W L_3$ -edge.

proximity to the much stronger band at 950 cm^{-1} suggest some caution in considering these data.

3.3. X-ray Absorption Spectroscopy. Experimental EXAFS $\chi(k)k^2$ signals at the $W L_3$, 7 and Ru K edges in pure WO_3 and mixed W-Ru oxide thin films are shown in Fig. 6. The Ru K-edge EXAFS signal was extracted only for WO_3 :16% Ru sample due to signal-to-noise limitations for other samples, having smaller Ru content. Note that all the $W L_3$ -edge EXAFS signals have close shape, that suggests a similarity of local environment around tungsten ions. The presence of well visible shoulder at 4.5 \AA^{-1} in tungsten EXAFS signals indicates that some high frequency contribution is present. It originates from outer co-ordination shells and so-called multiple-scattering (MS) events, related to multi-atoms correlation functions [6].

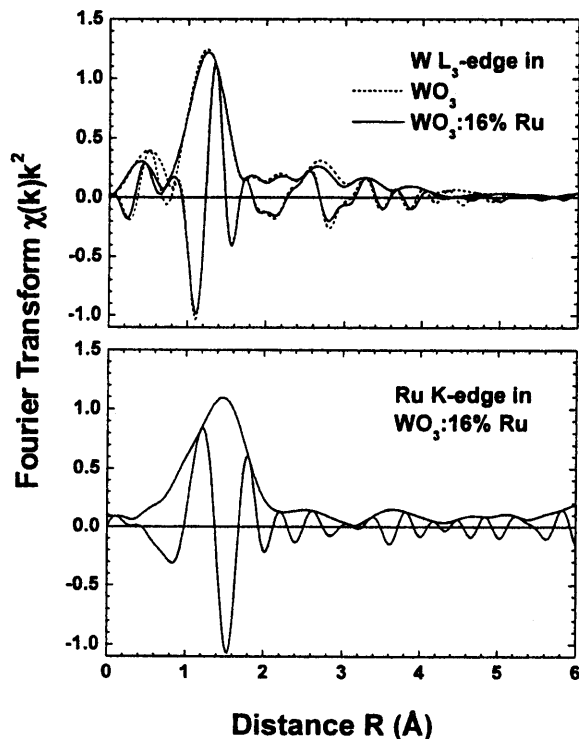


Fig. 7. Fourier transforms (FTs) of the experimental EXAFS $\chi(k)k^2$ signals at the $W L_3$ and Ru K edges in pure WO_3 and mixed WO_3 :16%Ru oxide thin films. Note that the positions of peaks in FTs do not correspond to the true crystallographic values, due to a phase shift present in the EXAFS signals.

On the contrary, the Ru K-edge EXAFS signal does not show any well defined high frequency signal, indicating that local environment around ruthenium ions is strongly disordered. These conclusions are supported by the Fourier transforms of the experimental EXAFS signals, presented in Fig. 7.

Only two FTs signals are shown for clarity in Fig. 7 for the tungsten edge. As one can see, a set of peaks is present in both samples and is well reproduced up to about 4 \AA . Based on our previous studies [19,20], these peaks are attributed to the single-scattering (SS) processes in the first coordination shell of tungsten ions formed by oxygens (the peak at $0.7\text{-}2.0\text{ \AA}$), to the MS contribution from the first shell (the peak at $2.2\text{-}2.9\text{ \AA}$) and to the complex contributions from the SS and MS signals in the second and third shells formed, respectively, by tungsten and oxygen ions (the peak at $2.9\text{-}4.2\text{ \AA}$). The EXAFS signals corresponding to the first peak in Fig. 7 were singled out by the back FT procedure and best-fitted using one-shell and two-shells models in the k -space range from 1.5 to 11.0 \AA^{-1} . The one-shell model assumes regular first coordination

shell of tungsten, i.e. that all oxygen atoms are located at the same distance. Thus it provided us with the average first coordination shell radius equal to about 1.8 Å. More precise information is given by the two-shells model, which takes into account a distortion of the first shell. The model suggests octahedral coordination of tungsten ions with a group of 4 nearest oxygen atoms at 1.78 ± 0.01 Å and two oxygen atoms at 2.04 ± 0.02 Å. The comparative analysis of the contribution of 4 nearest oxygen atoms at 1.78 Å shows that the distance increases of 0.01 Å under the doping that is in agreement with the decreasing of stretching mode from the value of 958 cm^{-1} for pure WO_3 film down to 932 cm^{-1} for Ru-doped samples.

The four nearest oxygen atoms are relatively strongly bound to central tungsten ion, as suggested by the small value of their Debye-Waller (DW) factors σ^2 , equal to about 0.002-0.004 Å². The remaining two oxygen ions are weakly bound and have the DW factors σ^2 equal to 0.007-0.010 Å². As a result, one can conclude that addition of ruthenium does not affect the short range order around tungsten ions.

The FT of the Ru K-edge EXAFS signal in mixed WO_3 :16%Ru film (Fig. 7) shows also some peaks beyond the first one. However, the noise present in experimental data and the absence of any well defined high frequency signal in the EXAFS signal (Fig. 6) allows to conclude that peaks in Fig. 7 beyond the first one have mainly the noise origin. The first peak at 0.5-2.1 Å is attributed to the first coordination shell of ruthenium. It was singled-out by the back-FT procedure and best-fitted by the one-shell model in the k-space range from 1.0 to 10.5 Å^{-1} . The obtained structural parameters suggest that ruthenium ions are six-fold coordinated by oxygen atoms with the mean R(Ru-O) distance equal to ~ 1.99 Å and the DW factor σ^2 equal to ~ 0.007 Å². Such coordination of ruthenium ions is quite close to that found in crystalline RuO_2 [21]. The absence of any detectable contribution from outer shells suggests that RuO_6 octahedra are weakly bound with surrounding films structure.

Thus, the EXAFS results suggest that the structure of mixed W-Ru oxide thin films is composed of WO_3 grains, having the structure close to that of pure WO_3 films, separated by disordered thin layers, containing ruthenium ions in the form of RuO_6 polyhedra.

4. Conclusions

The doping of tungsten trioxide films with foreign transition metals, in particular, ruthenium, during the sputte-

ring process seem to be a promising way to change the electrochemical reactivity and the optical properties of the films, without modifying appreciably the structure at the atomic level (coordination and bonds). In fact, the films still remain amorphous WO_3 films, and the basic electrochemical reactions are the same. A separate ruthenium oxide phase, in which ruthenium ions are six-fold coordinated with oxygen atoms, is also formed, closely surrounding or contacting anyway the grains of the tungsten trioxide matrix.

The insertion of ruthenium during the reactive sputtering seems to increase slightly the porosity of the films, but the main changes concern the electronic distribution at the interface between the WO_3 grains and ruthenium oxide disordered layer surrounded them. The electronic configurations on such interfaces allow optical transitions in the red light region and induce a remarkable resonant enhancement of the Raman scattering of the W-O terminal bond vibration, resembling similar previous findings in polycrystalline mixtures $\text{WO}_3\text{-ReO}_x$, also containing an electron donor transition metal oxide.

More detailed study on the chemical distribution and the electronic and optical properties of such doped films are under way, with a planned extension to other kinds of dopant metals.

5. Acknowledgements

This work was partially supported by MIUR (Italian Ministry of University and Research), in the framework of the research project "Piani di Potenziamento della Rete Scientifica e Tecnologica" Cluster No. 26-P4, and by the Latvian Government Research Grants No. 01.0811 and 01.0821.

We thank the LURE D21 beam line staff (Prof. S. Bénazeth, Dr. I. Nicolis, and Dr. E. Curis) for their technical collaboration. We also thank the "Laboratoire pour l'Utilisation du Rayonnement Electromagnétique" (LURE) for the beam time allocation and laboratory facilities.

6. References

- [1] S.K. Deb, Appl. Opt. Suppl. 3, 192 (1969).
- [2] K. Bange, Sol. Ener. Mater. & Sol. Cell 58, 1 (1999).
- [3] A. Kuzmin, Physica B 208&209, 175 (1995); A. Kuzmin, J. Physique IV (France) 7, C2-213 (1997).
- [4] V.L. Aksenov, A.Y. Kuzmin, J. Purans, S.I. Tyutyunnikov, Phys. Part. Nucl. 32, 675 (2001).

- [5] J.J. Rehr, J. Mustre de Leon, S.I. Zabinsky, R.C. Albers, *J. Am. Chem. Soc.* **113**, 5135 (1991); J. Mustre de Leon, J.J. Rehr, S.I. Zabinsky, R.C. Albers, *Phys. Rev. B* **44**, 4146 (1991).
- [6] A. Kuzmin, J. Purans, M. Benfatto, C.R. Natoli, *Phys. Rev. B* **47**, 2480 (1993); A. Kuzmin, J. Purans, *J. Phys.: Condens. Matter* **5**, 267 (1993).
- [7] C.-C. Hu, Y.-H. Huang, K.-H. Chang, *J. Power Sources* **108**, 117 (2002).
- [8] S. Trasatti, *Electrochim. Acta* **36**, 225 (1991).
- [9] A. Yamada, J.B. Goodenough, *J. Electrochem. Soc.* **145**, 737 (1998).
- [10] G.M. Ramans, J.V. Gabrusenoks, A.R. Lulis, A.A. Patamalnieks, *J. Non-Cryst. Solids* **90**, 637 (1987).
- [11] G.M. Ramans, J.V. Gabrusenoks, A.A. Veispals, *Phys. Status Solidi* **74**, K41 (1982).
- [12] J.V. Gabrusenoks, P.D. Cikmach, A.R. Lulis, J.J. Kleperis, G.M. Ramans, *Solid State Ionics* **14**, 25 (1984).
- [13] M.F. Daniel, B. Desbat, J.C. Lassegues, R. Garie, *J. Solid State Chem.* **73**, 127 (1988).
- [14] Y.S. Huang, F.H. Pollak, *Solid State Commun.* **43**, 921 (1982).
- [15] Y.S. Huang, P.C. Liao, *Sol. Ener. Mater. & Sol. Cell* **55**, 179 (1998).
- [16] L.-J. Meng, M.P. dos Santos, *Thin Solid Films* **375**, 29 (2000).
- [17] C. Vinegoni, M.Sc. Thesis, University of Trento (1996).
- [18] E. Cazzanelli, G. Mariotto, C. Vinegoni, A. Kuzmin, J. Purans, *Ionics* **5**, 335 (1999).
- [19] A. Balerna, E. Bernieri, E. Burattini, A. Lulis, A. Kuzmin, J. Purans, P. Cikmach, *Nucl. Instrum. Meth. A*, **308**, 234 (1991).
- [20] A. Kuzmin, J. Purans, *J. Phys.: Condens. Matter* **5**, 2333 (1993).
- [21] D.A. McKeown, P.L. Hagans, L.P.L. Carette, A.E. Russell, K.E. Swider, D.R. Rolison, *J. Phys. Chem. B* **103**, 4825 (1999).

Paper presented at the 9th EuroConference on Ionics, Ixia, Rhodes, Greece, Sept. 15 – 21, 2002.

Manuscript rec. Oct. 18, 2002; acc. Jan. 17, 2003.